Analysis of a Transonic Alternating Flow Phenomenon Observed during Ares Crew Launch Vehicle Wind Tunnel Tests

Martin K. Sekula[1] David J. Piatak[2] Russ D. Rausch[3]
NASA Langley Research Center, Hampton, VA 23681

Abstract

A transonic wind tunnel test of the Ares I-X Rigid Buffet Model (RBM) identified a Mach number regime where unusually large buffet loads are present. A subsequent investigation identified the cause of these loads to be an alternating flow phenomenon at the Crew Module-Service Module junction. The conical design of the Ares I-X Crew Module and the cylindrical design of the Service Module exposes the vehicle to unsteady pressure loads due to the sudden transition from separated to attached flow about the cone-cylinder junction with increasing Mach number. For locally transonic conditions at this junction, the flow randomly fluctuates back and forth between a subsonic separated flow and a supersonic attached flow. These fluctuations produce a square-wave like pattern in the pressure time histories which, upon integration result in large amplitude, impulsive buffet loads. Subsequent testing of the Ares I RBM found much lower buffet loads since the evolved Ares I design includes an ogive fairing that covers the Crew Module-Service Module junction, thereby making the vehicle less susceptible to the onset of alternating flow. An analysis of the alternating flow separation and attachment phenomenon indicates that the phenomenon is most severe at low angles of attack and exacerbated by the presence of vehicle protuberances. A launch vehicle may experience either a single or, at most, a few impulsive loads since it is constantly accelerating during ascent rather than dwelling at constant flow conditions in a wind tunnel. A comparison of a wind-tunnel-test-data-derived impulsive load to flight-test-data-derived load indicates a significant over-prediction in the magnitude and duration of the buffet load.

Note To Readers

The predicted performance and certain other features and characteristics of the Ares I and Ares I-X launch vehicles are defined by the U.S. Government to be Sensitive But Unclassified (SBU). Therefore, details have been removed from all plots and figures.

I. Introduction

One of the many buffet events that can be encountered by a launch vehicle during assent is a transition of flow from a subsonic to a supersonic flow state at expansion corners created by vehicle geometry changes such as cone-cylinder junctions. This event can create a large, abrupt pressure change directly aft of a cone-cylinder junction resulting in potentially significant, impulsive loads. The quasi-steady nature of wind tunnel testing causes this transonic event to manifest itself as an alternating flow separation and attachment phenomenon where the flow

[1] Research Engineer, Aeroelasticity Branch, Mail Stop 340
[2] Research Engineer, Aeroelasticity Branch, Mail Stop 340
[3] Research Aerospace Engineer, Aeroelasticity Branch, Mail Stop 340

fluctuates between a separated subsonic flow and an attached supersonic flow. These random fluctuations between the two flow states result in large, abrupt surface pressure changes whose time histories resemble a square wave. These square-wave-like pressure time histories produce large buffet loads when integrated around the model circumference.

This alternating flow phenomenon is well documented in launch vehicle buffet literature[1-6]. Chevalier and Robertson describe the conditions required for the onset of alternating flow and the physics resulting in the sustained fluctuation between the two flow states:

> "The attachment of the flow begins when the momentum of the flow aft of the shoulder [cone-cylinder junction] directed toward the cylinder is sufficient to support attachment. The momentum component directed towards the surface is indicated by the overexpansion in this region. This attachment results in a large increase in local Mach number at the shoulder and a corresponding large adverse pressure gradient to decelerate the flow back to free-stream conditions. The boundary layer cannot withstand this gradient and separates at some distance downstream of the shoulder. This local separation being in a supersonic flow field produces a near normal shock wave, and the accompanying large back pressure feeds forward to the shoulder. The resulting forward progression of the separation point can cause the flow to revert to the initial separated flow conditions. With the original conditions established the cycle starts again with attachment."[1]

This alternating separation and attachment flow event was encountered[7] during transonic buffet investigations of the Ares I family of launch vehicles at NASA Langley's Transonic Dynamics Tunnel (TDT)[8-11]. For these investigations, rigid, geometrically-scaled (3.5 percent) wind-tunnel models of the Ares I-X Flight Test Vehicle (FTV) and Ares I Crew Launch Vehicle were designed, fabricated, and furnished with a suite of sensors. Both models were instrumented with a large number of miniature unsteady pressure transducers located in the vicinity of the region affected by the alternating flow phenomenon providing a unique opportunity to examine this phenomenon using a much greater sensor density and higher sample rate than previously available.

The goal of these tests was to develop buffet forcing functions that are used by the Ares program to predict vehicle loads and responses due to transonic buffet phenomena. Although the analysis of the alternating flow phenomenon is only a subset of the test goals, it is the primary focus of this paper. In particular, the paper will describe the methods developed to model the alternating flow in the Ares I-X buffet forcing functions and to provide additional insight into this phenomenon based on the acquired test data.

II. Background

A. Test description

Two 0.035-scale Rigid Buffet Models (RBM) of the Ares I-X and Ares I launch vehicles, presented in Figure 1, were tested at NASA Langley's Transonic Dynamics Tunnel to assess the transonic buffet environment. The TDT, depicted in Figure 2, is a 16-foot-by-16-foot test section, closed-circuit, continuous flow wind tunnel built for the purposes of conducting aeroelastic research and of clearing vehicles of aeroelastic phenomena such as flutter. The TDT is capable of testing over a range of stagnation pressures from near vacuum to atmospheric and Mach numbers from near zero to 1.2 in both air and R134a heavy gas test medium.

(a) Ares I-X (b) Ares I

Figure 1. Rigid Buffet Models installed in the TDT test section.

The models developed for this project were rigid, not aeroelastically scaled. Each model was instrumented with 256 miniature unsteady pressure transducers embedded in the model skin in rings of four or eight transducers along the length of the model to record time correlated unsteady surface pressure responses. Each data record consisted of 30 second time histories acquired at a 12 KHz sample rate, with a 4.5 KHz anti-aliasing filter. The models were

tested with and without protuberances, at Mach conditions ranging from 0.8 to 1.2 in air and R134a heavy gas test mediums. For each Mach number, the effect of model attitude on buffet was assessed by obtaining data at combinations of model pitch and roll angles of -8 to 8 degrees and -180 to 180 degrees, respectively. Further discussion of Ares I-X and Ares I buffet testing and analysis can be found in References 8 through 11.

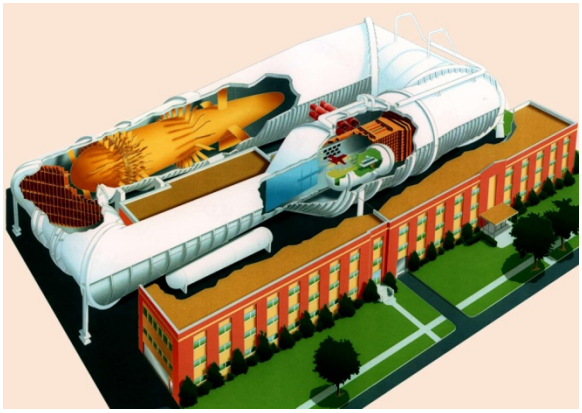

Figure 2. NASA Langley's Transonic Dynamics Tunnel.

B. Buffet Forcing Function Development

Buffet Forcing Functions (BFFs) are a series of orthogonal force time histories acting at the centerline of a launch vehicle model (see Figure 3). These time histories represent the unsteady aerodynamic loads acting on each segment of the model. The loads are obtained by integrating measured pressures from rings of transducers distributed along the longitudinal axis of the model.

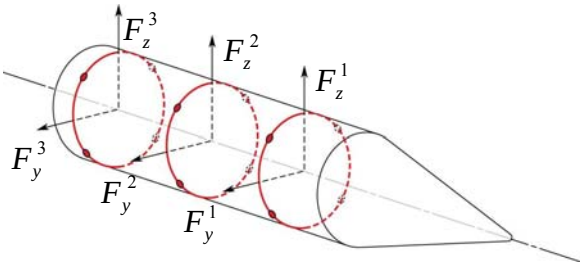

Figure 3. Forcing functions acting on the centerline of a model.

The BFFs can be calculated using two methods of pressure integration yielding either sectional (force/length) or point (force) loads - each useful for different types of analyses. Sectional loads, depicted in Figure 4a, are calculated by integrating the measured pressures along the circumference at the station where they were measured. These BFFs have units of force-per-length and are useful for comparing the relative strength of the buffet loads at various vehicle stations. Point forces, portrayed in Figure 4b, are calculated by integrating the measured pressures circumferentially and longitudinally over a segment of the model. Loads calculated through this method are used to conduct the buffet loads analysis and represent the total buffet load acting on a segment of the vehicle. The subject matter of this paper dictates that the sectional loads, or force-per-length loads, are used through most of the paper.

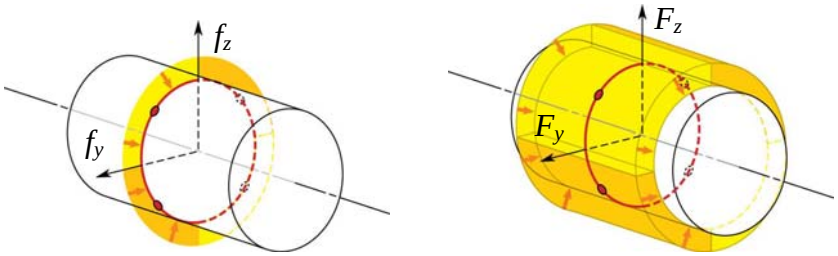

(a) Sectional load integration. (b) Point load integration.

Figure 4. Loads resulting from two methods of pressure integration.

C. Manifestation of Alternating Flow

Figure 5 presents a sample surface pressure time history measured by a transducer placed near the Crew Module (CM)-Service Module (SM) junction, an expansion corner on the upper stage of the Ares I-X, that can be seen in the photograph in Figure 6. The large abrupt jumps in the pressures indicate the change of flow states from a separated, subsonic flow to an attached, supersonic flow or vice versa. The occurrences of these jumps are random and appear not triggered by model dynamics or facility phenomena such as free-stream pressure fluctuation due to tunnel drive blade passage.

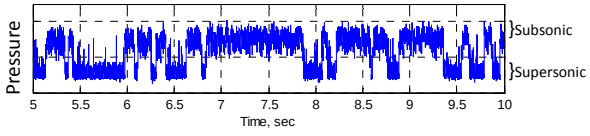

Figure 5. Sample pressure time history of alternating flow.

The aerodynamic phenomenon causing these abrupt changes in the surface pressure was also observed using shadowgraphs, a qualitative visual measurement technique. Figures 7(a and b) present two shadowgraphs of the flow expansion at the CM-SM junction identifying the distinct shock structures associated with the two flow states. The location on the Ares I-X vehicle where these shadowgraphs were acquired is identified by a box on the vehicle schematic in Figure 7. The dark region at the top of each figure is the shadow of the lower half of the Ares I-X Launch Abort System (LAS), CM, and SM projected onto the far wall of the TDT test section using a high intensity light source shone through the control room windows. A red line was added to the figure to accentuate the outline of the model. The flow in both figures is from the right to the left and emanating from the bottom of the Ares I-X outline are shadows of shock waves created by the flow around the expansion corner. Figure 7a presents the shock structure existing near the expansion corner when the flow traverses the corner in a separated, subsonic state. A weak shock is emanating from the expansion corner and a faint terminal shock can be identified further downstream. At some distance off the surface the two shocks can be seen to join together. Figure 7b presents the shock structure created by supersonic flow around the expansion corner. An expansion fan shock is present at the corner and an oblique shock is visible downstream of the expansion fan. Further down the vehicle, a stronger terminal shock than the one found in Figure 7a can be seen. It emanates from the vehicle and combines with the oblique shock at some distance off the vehicle surface. These two shock structures at the expansion were also noted during a CFD analysis of this problem[6].

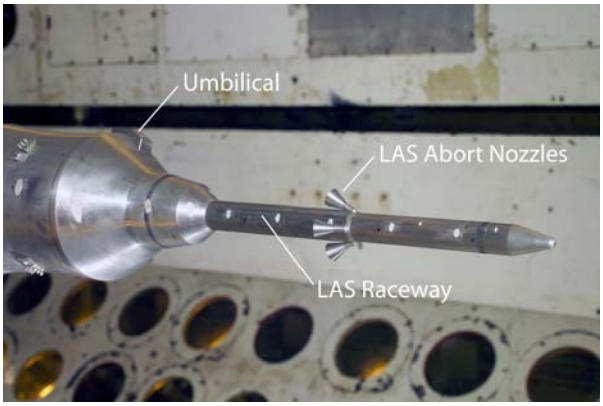

Figure 6. Close-up of the Crew Module/Service Module junction on the Ares I-X RBM.

(a) Subsonic, detached flow (b) Supersonic, attached flow

Figure 7. Shadowgraph of the Ares I-X RBM shock structure at the expansion corner, protuberances on.

III. Development of Tools for Identification and Analysis of Alternating Flow

A. Identification of Alternating Flow in Test Matrix

Buffet forcing functions were developed for a range of Mach numbers and a series of model attitudes which span the predicted trajectories of both the Ares I-X and Ares I. Since numerous test conditions exist were the alternating flow phenomenon may be present, a method was needed to help identify these test conditions.

The two flow states in alternating flow have significantly different mean pressures and the change between the two states is very abrupt. These pressure jumps result in very large root-mean-square (rms) values for the time histories and therefore can be used to identify flight conditions affected by this phenomenon.

Figure 8(a-b) presents a color intensity plot of the peak rms value of the fluctuating component of the pressure coefficient, $\Delta C_{p,rms}$, measured on the model as a function of model pitch angle and Mach number for (a) Ares I-X and (b) Ares I RBMs. Figure 8a indicates a region of high $\Delta C_{p,rms}$ values in the vicinity of Mach 0.9, suggesting the presence of alternating flow. This figure also indicates that the alternating flow occurs at higher Mach numbers as model pitch is increased. This influence of model pitch on the critical Mach number is substantiated by a previous study that noted the same observation[1]. The Mach number at which the high $\Delta C_{p,rms}$ region occurs seems to show

some asymmetric dependence on model pitch. A probable source of this asymmetry is the presence of a large protuberance, the CM-SM umbilical, on the Ares I-X RBM at the cone-cylinder/CM-SM junction.

Ares I maximum $\Delta C_{p,rms}$ as a function of Mach number and model pitch is presented in Figure 8b. As in the Ares I-X data, the peak $\Delta C_{p,rms}$ levels increase near Mach 0.9, but the maximum fluctuating pressures are significantly smaller than those experienced by the Ares I-X at the same test conditions. This reduction in pressure coefficient rms levels can be attributed to a change in vehicle design - using an ogive fairing in lieu of a cone-cylinder junction. The increase at Mach 0.9 in $\Delta C_{p,rms}$ is created by a terminal shock moving across the surface of the ogive fairing. The second region of high $\Delta C_{p,rms}$ levels occurs between Mach 0.95 and 1. This increase is caused by a shock wave located at the frustum of Ares I. Neither of these events is associated with an alternating flow phenomenon. The geometric changes made as the design matured from the Ares I-X to the Ares I configuration eliminated the conditions required for the onset of alternating flow separation and attachment phenomenon.

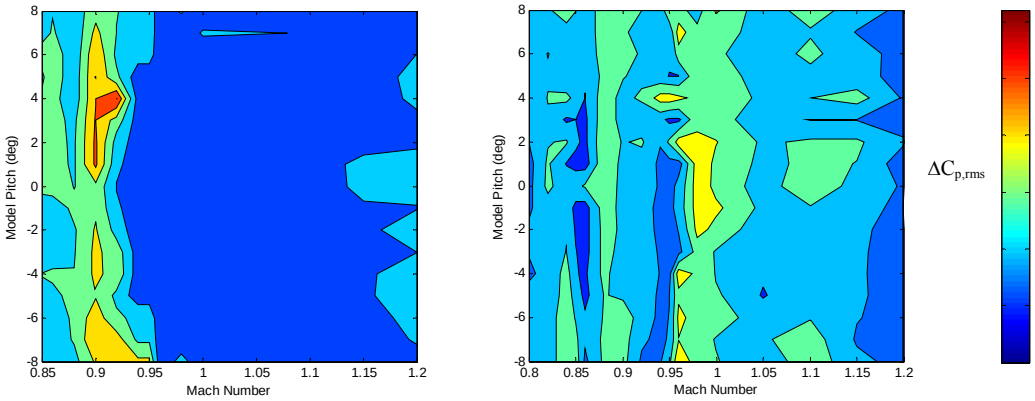

(a) Ares I-X (b) Ares I

Figure 8. Contour plot of peak $\Delta C_{p,rms}$ versus model pitch and Mach number, protuberances on.

B. Analysis of Pressure Time Histories

Figure 9 presents the time histories of pressures measured by a ring of eight transducers just downstream of the expansion corner formed by the Ares I-X CM-SM junction at a test condition of Mach 0.9 and 0 degrees model pitch and roll. The time histories of 7 out of the 8 transducers indicate the presence of alternating flow. A low-pass filter was employed to eliminate the higher frequency content of the time histories, thereby more clearly identifying the (running) mean pressure jumps associated with the changes in flow state (see green trace in Figure 9). A closer examination of Figure 9 indicates that adjacent transducers often change their mean pressures almost simultaneously. Transducers at azimuth angles 270, 315, and 0 degrees display a close relationship in the flow state across these three transducers. Likewise, the pressures measured by transducers at azimuth angles 45, 90, 135, and 180 degrees generally tend to change states together. Furthermore, even though the flow states at azimuths 0 and 45 degrees are different, the pressure time histories indicate a level of interdependency of the local flow fields at the two transducers. The fluctuating pressures indicate a near simultaneous, but opposing change in the flow states at the two locations (see Figure 9, events at t=3 sec and t=14 sec).

A closer examination of the start times of these near simultaneous pressure changes measured at 0 and 45 degree azimuth was conducted to identify which region of the circumference first transitions from one flow state to the other. Events were identified in both pressure time histories where a pressure jump in one time history was found to precede a pressure jump in the other time history. This observation indicates that the change in flow state at either transducer can precipitate a change in flow state at the other transducer.

Histograms were used to identify alternating flow events in the pressure time histories. Figure 10 presents the histograms of the pressure time histories presented in Figure 9. Unlike a typical, random pressure fluctuation that has a Gaussian distribution, alternating flow histograms exhibit a double peak distribution. This double peak distribution is found in most of the histograms associated with the pressure time histories in Figure 9. The relative amplitudes of the peaks are an indication of the prevalence of each flow state.

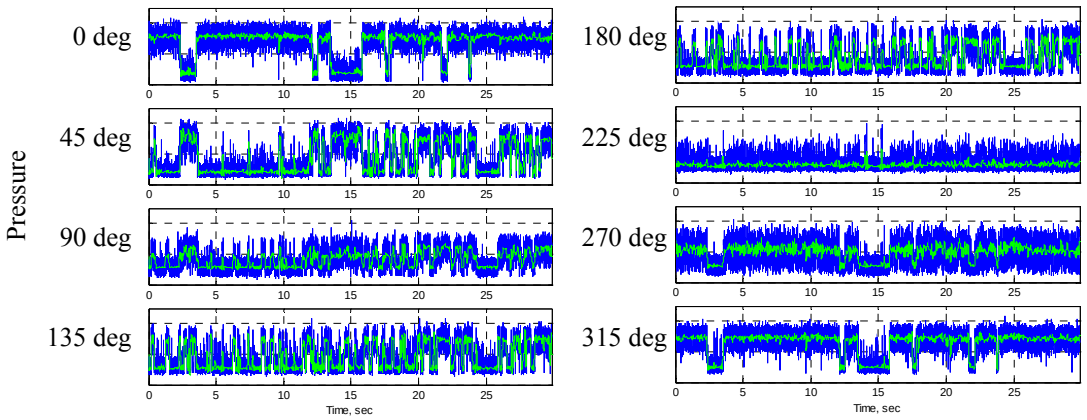

Figure 9. Pressure time histories at CM-SM junction, M=0.9, pitch=0°, roll=0°, protuberances on. Unfiltered time histories (blue), low-pass filtered time histories (green).

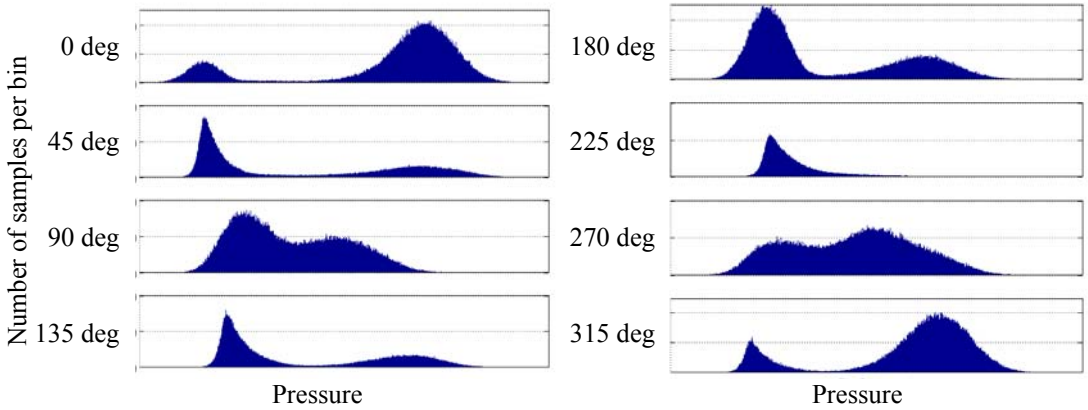

Figure 10. Histogram of pressure time histories at CM-SM junction, M=0.9, pitch=0°, roll=0°, protuberances on.

Figure 11 present histograms of the pressure time histories measured by the same transducers, but at a model angle of attack of 4 degrees. The histograms indicate that the transducer at model azimuth angle of 135 degrees is experiencing pressure fluctuations created by an alternating flow. The adjacent locations (90° and 180°) exhibit a non-Gaussian distribution of pressure data, indicating the presence of some other aerodynamic phenomenon. A closer examination of the pressure time histories (not presented) points to a combination of shock fluctuation mixed with a less frequent occurrence of jumps between the two flow states. The histograms of pressures at 270, 315, 0, and 45 degree azimuth angles (leeward side of the model) have Gaussian distributions at pressures indicative of a separated, subsonic flow.

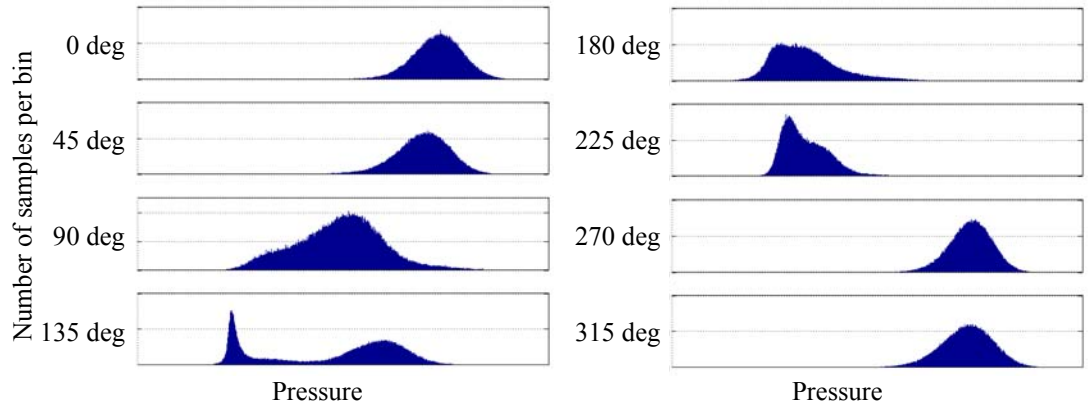

Figure 11. Histogram of pressure time histories at CM-SM junction, M=0.9, pitch=4°, roll=0°, protuberances on.

The above discussion identifies alternating flow events using a histogram technique, but it does not indicate whether the phenomenon occurs simultaneously across multiple transducers. The cross-correlation function between two pressure time histories provides a measure of similitude between the two pressures. Random pressure fluctuations typically have very low coherence as a function of azimuth, and therefore result in low cross-correlation values. Alternating flow is a phenomenon that dominates pressure time histories resulting in high cross-correlation values, if observed at multiple transducer locations. This characteristic can be exploited to identify potential alternating flow events that span multiple transducer locations around the circumference of the model.

Figure 12 presents a polar plot of the maximum cross-correlation of each pressure time history in Figure 9 with every other pressure time history at that model station as a function of azimuth angle. The radial coordinate of the polar plot represents the cross-correlation of two pressure time histories ranging from 0 to 1, where the center of the polar plot represents a cross-correlation of 0, or no similitude, and the outer circumference represents a value of 1, or complete similitude. The polar coordinate represents the azimuth angle of the 8 transducers on the model. In order to provide a better understanding of the data presented in this figure, the maximum cross-correlation of pressures at 0 degrees with respect to the other pressures is represented by the green line in Figure 12. Pressures at azimuth angles 270 and 315 degrees have a high cross-correlation, greater than 0.5, with respect to the pressure at 0 degrees azimuth. The cross-correlation with the remaining pressures is low, less than 0.2. Seven more sets of maximum cross-correlation functions are calculated, one for each of the other seven pressure time histories measured at this model station. These cross-correlation functions are overlaid to create a plot identifying which locations around the circumference have similar time histories. Locations of pressures with high cross-correlation values (greater than 0.5) are highlighted with thicker lines; otherwise the line thickness is reduced (see Figure 12, 225 degree azimuth angle). The line color is also changed to group together locations whose pressure time histories have a high cross-correlation.

Figure 12 confirms the previous, qualitative discussion of the pressure time histories presented in Figure 9, surmising that two circumferential regions exist where flow around the expansion corner tends to simultaneously change states: azimuth angles of 270, 315, and 0 degrees and azimuth angles of 45, 90, 135, and 180 degrees. Although alternating flow can be limited to an area encompassing only a single transducer, and thereby not identified through this technique, larger areas of alternating flow, detected at multiple locations, are of higher importance due to the magnitude of the loads that they can impart on the vehicle.

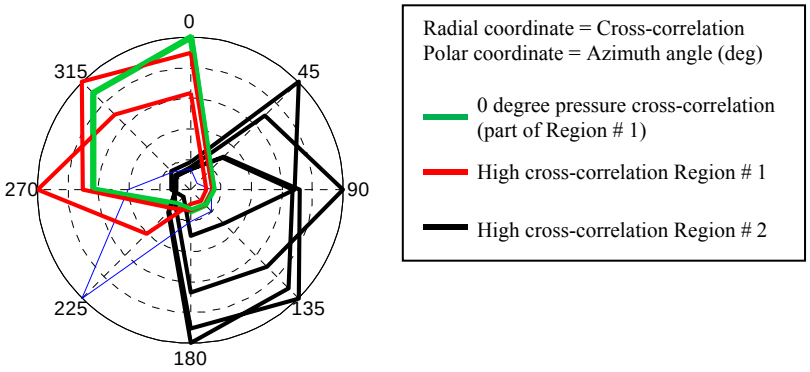

Figure 12. Maximum cross-correlation of pressures at CM-SM junction, M=0.9, pitch=0°, roll=0°, protuberances on.

IV. Analysis of Alternating Flow Data

The two aforementioned alternating flow identification techniques, along with $\Delta C_{p,rms}$ values, were used to examine the effect of model pitch and protuberances on the presence of the alternating flow phenomenon. Unless stated otherwise, all the data presented in the following sections is for a station of transducers just downstream of the CM-SM junction at 0.9 Mach number. This station and this Mach number were chosen because they exhibit the most intense examples of the alternating flow phenomenon.

A. Protuberances on configuration

Figure 13 presents the maximum cross-correlation between pressure time histories at Mach 0.9 for model pitch angles ranging from -8 to 8 degrees and 0 degree model roll angle. Figure 13a presents cross-correlation polar plot for a 0 degree pitch case, while Figures 13(b-f) present the same data for positive model pitch angles, and Figures 13(g-k) for negative pitch angles. For positive pitch angles, the windward side of the model is at 180 degrees azimuth, while for negative pitch angles the windward side is at 0 degree azimuth. The general location of the alternating flow phenomenon shows little sensitivity to small (1 degree or smaller) pitch attitudes regardless of sign

(Compare Figures 13(a,b, and g)). For positive and negative 2 degree pitch angles, the alternating flow migrates to the windward side of the model. This tendency of the alternating flow to favor one side of a vehicle over another has been noted by Chavalier and Robertson[1]. Reference 1 also confirms that the alternating flow sets up on the windward side of models with expansion corner geometries similar to the one found on the Ares I-X. Above two degrees of pitch (nose-up or nose-down), the location of the high cross-correlation regions is asymmetric indicating that protuberances, LAS nozzles and CM-SM umbilical, influence the local flow field.

The cross-correlation results and insight garnered from histograms (not shown) indicate that the relatively high cross-correlation values found at pitch angles greater than 4 degrees nose-up are not caused by an alternating flow. This observation was confirmed by examining the pressure time histories, which display characteristics more typical of a standing shock. The fact that the high cross-correlation is not caused by alternating flow does not denote its absence. Alternating flow still occurs at model pitch angles above 4 degrees, but it is not correlated across multiple transducers.

Figure 14 presents a color intensity plot of the $\Delta C_{p,rms}$ values of pressure time histories as a function of model pitch angle and azimuthal station. This figure indicates that at small model pitch angles (-1 through 1 degree) there are large circumferential areas of significant pressure fluctuation, indicative of the presence of alternating flow. The highest $\Delta C_{p,rms}$ values occur between 0 and 45 degrees, in the vicinity of the CM-SM umbilical. The pressure time histories presented in Figure 9 indicate that the large $\Delta C_{p,rms}$ values are produced by pressure jumps caused by the alternating flow. Increasing the model pitch, both in the positive (nose-up) or negative (nose-down) direction generally reduces the $\Delta C_{p,rms}$ values. For positive pitch angles, alternating flow occurs at 135 degree model azimuth, while for negative pitch angles it occurs in the 225 to 270 degree azimuth range.

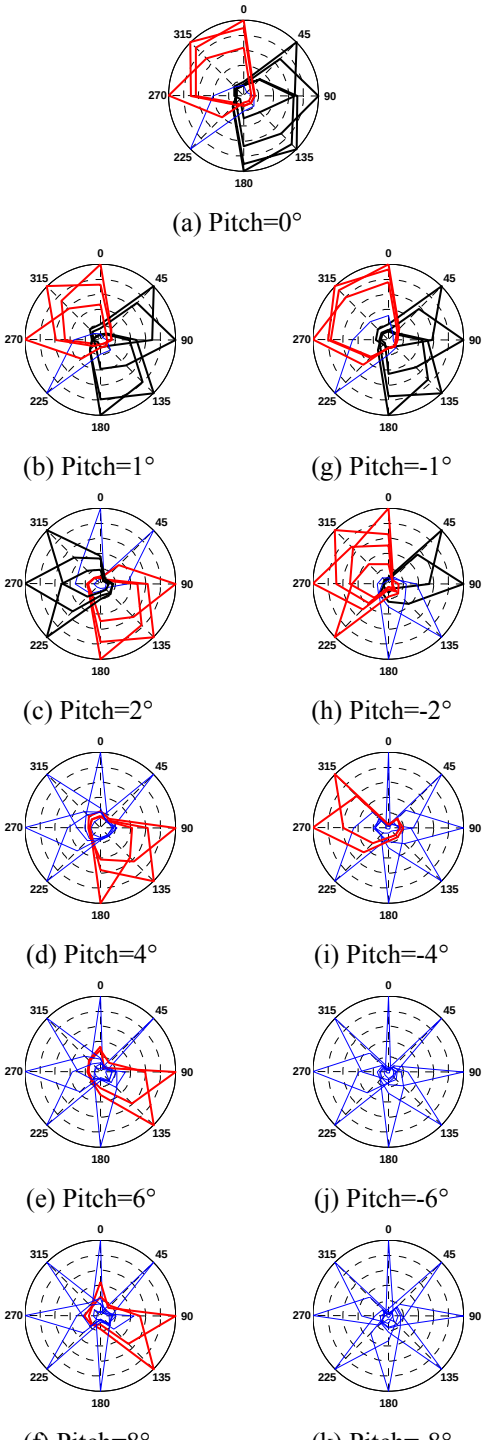

Figure 13. Maximum cross-correlation of pressures as a function of model pitch angle, M=0.9, roll = 0°, protuberances on.

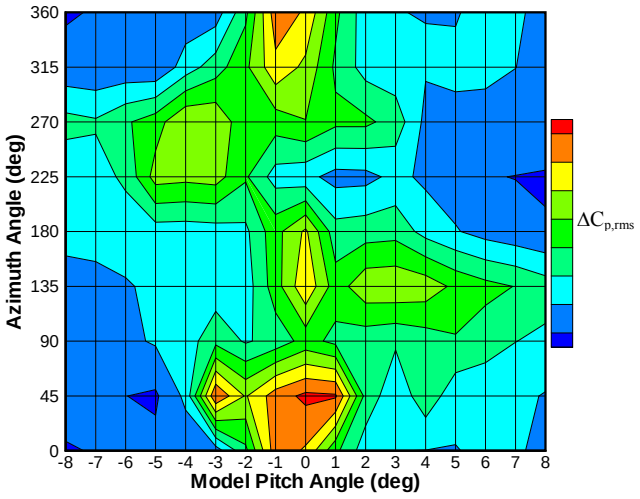

Figure 14. Measured $\Delta C_{p,rms}$ as a function of model pitch angle and transducer azimuthal location, M=0.9, roll = 0°, protuberances on.

B. Protuberance off configuration

The RBMs were designed with removable protuberances in order to be able to ascertain the contribution of the protuberances to the buffet loads. A protuberance off, or clean, configuration was tested at a limited range of Mach numbers which included Mach 0.9. For the Ares I-X model, the removed protuberances that could affect the alternating flow phenomenon included the CM-SM umbilical and the abort motor nozzles (see Figure 6.) The LAS raceway was a permanent feature of the model which could potentially affect the flow at the command module.

Figure 15 presents the maximum cross-correlation of pressures polar plots as a function of model pitch angle for the protuberance off configuration of the Ares I-X RBM. As the model is pitched above 1 degree (positive and negative), the alternating flow tends to move to the windward side of the model (180 degree azimuth for a positive pitch, 0 degree azimuth for negative pitch.) There is an asymmetry present in the cross-correlation dependant on positive or negative model pitch. The source of this asymmetry is unknown; several possible causes exist including model eccentricity, the non-removable LAS raceway protuberance, and tunnel flow angularity.

The effect of protuberances on pressure time history cross-correlation as a function of positive model pitch angles was examined by comparing Figures 15(b-f) and 13(b-f). The largest changes in cross-correlation occur at 1 and 2 degrees pitch angles. At 1 degree model pitch angle a region of alternating flow centered at 315 degrees for the protuberance on configuration shifts to the windward side of the model (225-270 degrees) for the protuberance off configuration and at 2 degrees model pitch this region of alternating flow disappears altogether for the protuberance off configuration. At model pitch angles of 4 and 6 degrees, a region of correlated flow at 225-270 degree azimuth is present again, but an examination of the time histories and their histograms indicates the high cross-correlation is caused by a terminal shock, not alternating flow.

Flow cross-correlation at negative model pitch angles is significantly affected by the presence of protuberances. Figures 15(g-k) indicate that a large, correlated alternating flow region occurs on the windward side of the protuberance off model. This region is not present when protuberance are installed (See Figures13(g-k)). This difference is more than likely cause by the presence of the large CM-SM umbilical protuberance on the windward side of the model.

Figure 16 presents a color intensity plot of the $\Delta C_{p,rms}$ values for measured pressure time histories as a function of model pitch angle and azimuthal station for the protuberance off configuration of the Ares I-X RBM. At positive pitch angles, the transducer at azimuth angle 135 degrees measures large $\Delta C_{p,rms}$ values while for negative pitch angles, the transducer at 0 degree azimuth angle measures large $\Delta C_{p,rms}$ values. Both of these transducers are measuring pressure fluctuations caused by alternating flow. One would expect the location of the alternating flow to be symmetric (0 and 180 degrees) as the model is pitched in the positive and negative direction. The cause of

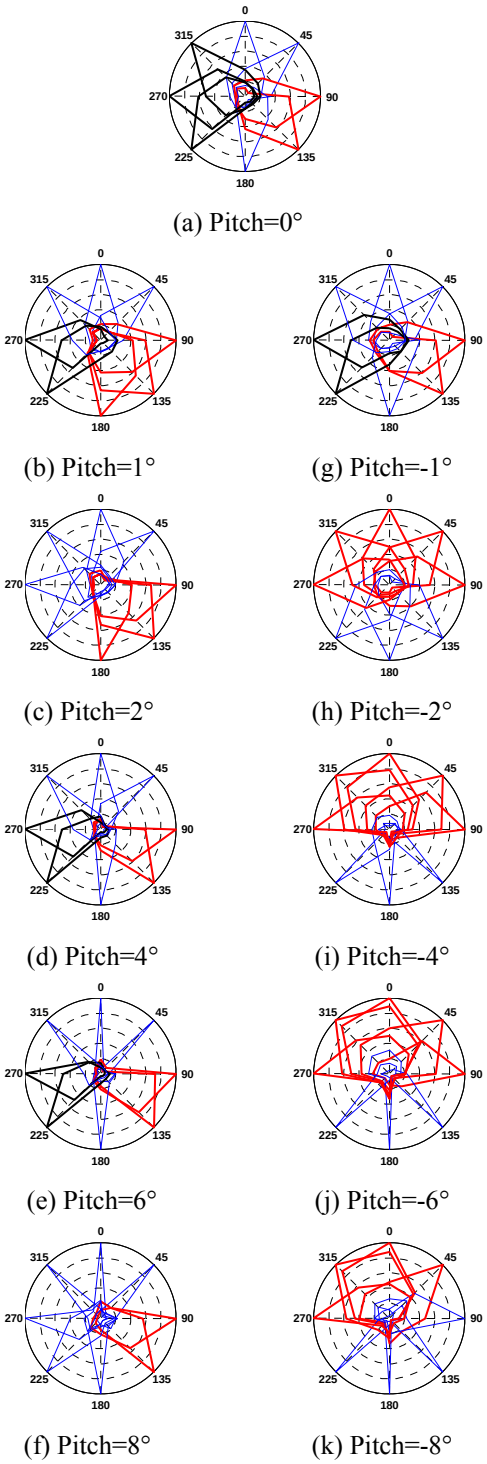

(a) Pitch=0°

(b) Pitch=1° (g) Pitch=-1°

(c) Pitch=2° (h) Pitch=-2°

(d) Pitch=4° (i) Pitch=-4°

(e) Pitch=6° (j) Pitch=-6°

(f) Pitch=8° (k) Pitch=-8°

Figure 15. Maximum cross-correlation of pressures as a function of model pitch angle, M=0.9, roll = 0°, protuberances off.

this asymmetry is unknown.

The differences between Figures 13 and 15, particularly on the 0 degree azimuth side of the model indicate that the presence of protuberances plays a significant role in the flow dynamics at the CM-SM junction. The earlier discussion of Figure 9 concluded that the two regions of alternating flow tend to be 180 degrees out of phase with respect to each other with the boundary between the two regions occurring at the CM-SM umbilical. The impact of the CM-SM umbilical on the location of the alternating flow regions is further investigated in Figure 17. This figure presents the maximum cross-correlation of pressures polar plots for four model attitudes, where the pitch angle was held at 0 degrees and the model was rolled. The regions of high pressure cross-correlation generally do not move around the model circumference as a function of model roll angle, particularly the region ranging from 225 to 0 degrees azimuth. This observation suggests that the boundary of at least one of the regions of alternating flow may be fixed azimuthally in the 0 – 45 degree region by the large the CM-SM umbilical protuberance. Unfortunately, this observation could not be substantiated due to the lack of similar data for the protuberance off model configuration.

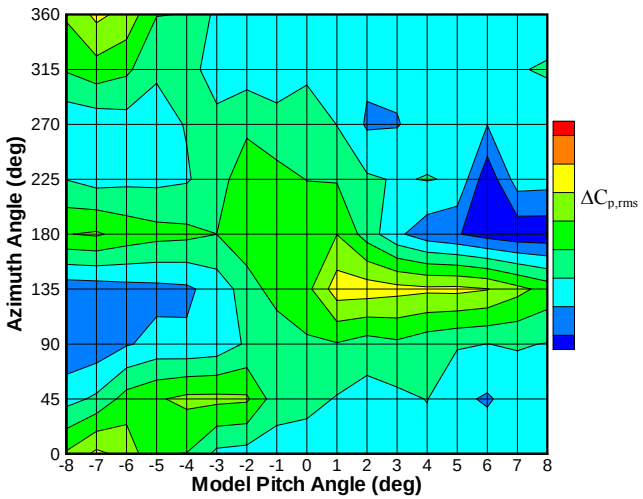

Figure 16. Measured $\Delta C_{p,rms}$ as a function of model pitch angle and transducer azimuthal location, M=0.9, roll = 0°, protuberances off.

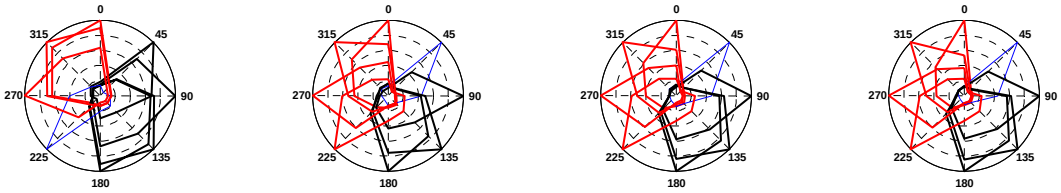

(a) roll=0° (b) roll=90° (c) roll=180° (d) roll=270°

Figure 17. Maximum cross-correlation of pressures as a function of model roll angle, M=0.9, pitch = 0°, protuberances on.

C. Downstream Effects of Alternating Flow

Figure 18 presents pressure time histories measured by transducers downstream of the CM-SM junction located at a single model azimuth (0 degrees), at a model attitude of 0 degrees pitch and roll. The extent of downstream influence of alternating flow is visible in this figure. An alternating flow event was measured at approximately 19.7 seconds. The event is present in the pressures measured at stations 1 through 6, spanning a distance of approximately 1.3 model diameters downstream of the expansion corner. An examination of pressure time histories at model pitch angles ranging from -8 to +8 degrees (not presented) indicates that for most model pitch angles, the impact of alternating flow was detected by the first 6 transducers downstream of the expansion corner. Since the next transducer, station 7, was 1.7 model diameters downstream from the expansion corner, it impossible to ascertain from this data a more accurate extent of downstream influence of alternating flow.

The pressure time histories in Figure 18 indicate that the measured pressure changes due to alternating flow act differently depending on longitudinal model station. Comparing stations 1 and 3, alternating flow results in an increase in static pressure at station 1, and a decrease at station 3. This trend in the alternating flow pressure change as a function of model station was also observed by Chevalier and Robertson[1]. These changes in pressure are directly related to the static pressures for an attached supersonic flow and a separated subsonic flow.

Figure 19a presents the static pressures for transducers 1 through 8 at Mach numbers 0.88 and 0.92, bounding Mach conditions at which the flow at the CM-SM junction remains either a separated, subsonic flow or an attached, supersonic flow, respectively. The locations of the transducers on the Ares I-X outer mold line is presented in Figure 19c. The attached flow static pressures at transducers 1 and 2 are lower than the corresponding separated flow static pressures, but for transducers 3 through 5, the separated flow static pressure is lower. The relative

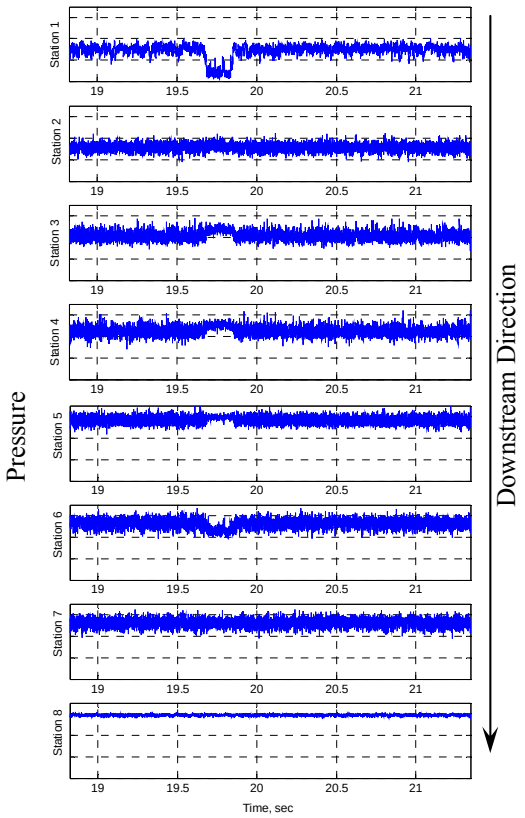

Figure 18. Pressure time histories measured downstream of CM-SM junction at 0 degree azimuth, M=0.9, pitch=0°, roll=0°, protuberance on.

pressure magnitudes reverse again at transducer 6, which is not noted by Chevalier and Robertson, and most likely influenced by the vicinity of another expansion corner located just aft of transducer 6.

Figure 19b compares the differences between the static pressures at Mach 0.88 (separated) and 0.92 (attached) to the difference between the Mach 0.9 static pressures in the attached and separated flow states. Except at transducer 2, the corresponding differences compare well, raising the possibility that wind tunnel data from Mach numbers just below and just above the alternating flow Mach number may be used to accurately predict and bound the overall magnitude of loads produced by this phenomenon.

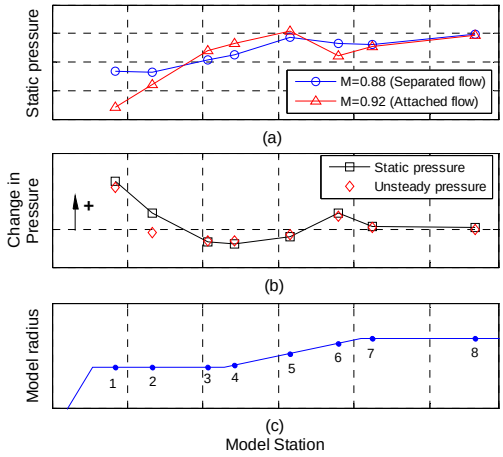

Figure 19. Relationship between static pressures at M=0.88 and 0.92 and the alternating flow pressure amplitude at M=0.9, pitch=0°, roll=0°, protuberance on.

V. Flight Test Buffet Forcing Functions

A. Modeling of Alternating Flow

The alternating flow phenomenon created a unique challenge in the analysis of the Ares I-X buffet loads. The large abrupt pressure changes, when integrated over the surface of the vehicle, produce extremely large fluctuations in the BFFs. Data from the two wind tunnel investigations of transonic buffet are long time records of unsteady pressures acquired at constant Mach numbers. This constant Mach condition is not representative of a launch velocity profile, where a vehicle is continuously accelerating. Keeping the velocity constant provides the flow with the opportunity to indefinitely switch back and forth between the separated and attached flow states. The multiple, square-wave-like changes in the surface pressures, when integrated, produce a series of impulsive loads presented in Figure 20a. These multiple impulsive loads result in unrealistically high buffet loads. The short duration that the launch vehicle spends in the critical Mach range conducive to alternating flow suggests that, most likely, only a single change in flow states may occur[4]. Therefore, a method of modeling a single alternating flow event in the buffet forcing functions was developed.

Based on the assumption that only a single impulse would occur, a procedure was developed to model this single impulse using wind tunnel data. The procedure uses the integrated point loads instead of individual pressure time histories. First, a low-pass filter is applied to the point load time histories at stations affected by alternating flow. Next, the largest impulsive load created by alternating flow is identified based on the root-mean-square value of a fixed length window propagated across the entire filtered time history. In order to increase the conservatism of the analysis, the window size was chosen to excite the vehicle first bending mode.

Once the largest impulsive load event is identified, the point load time histories for all the vehicle stations affected by alternating flow are low-pass filtered and all other impulsive load events in the time histories are removed. These filtered time histories containing only that single event are superimposed on the point load time

histories obtained at Mach conditions just above and below the critical Mach number resulting in point load time histories such as the one presented in Figure 20b. These two Mach numbers exhibit either pure subsonic, separated flow or supersonic, attached flow characteristics. This "book ending" of the alternating flow critical Mach number is employed to examine the effect of unsteady subsonic separated and supersonic attached flow signal content on vehicle buffet response during the transition between the two flow states.

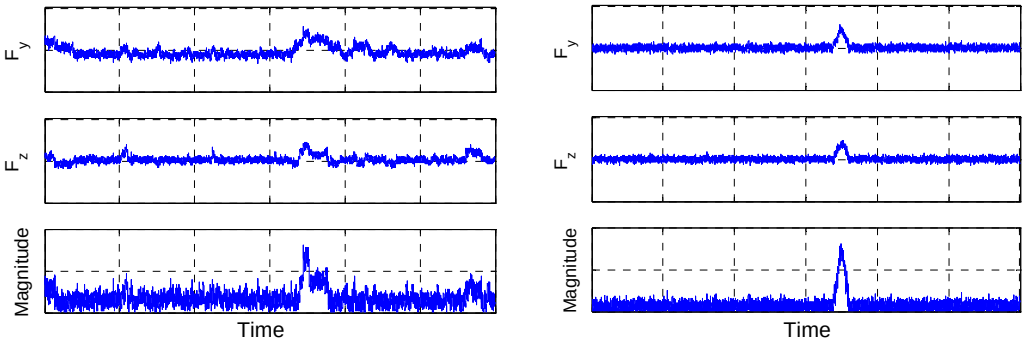

(a) Unfiltered, multiple event (b) Filtered, single event

Figure 20. Buffet forcing functions just aft of the expansion corner, M=0.9, pitch=1°, roll=0°, protuberance on.

B. Ares I-X Flight Data Comparison

Figure 21 presents the magnitude and direction of the integrated load time histories produced by the change from subsonic to supersonic flow based on (a) wind tunnel predictions (α=1° and β=0°) and (b) Ares I-X flight test measurements (α=0.2° and β=-0.9°). The direction of the load is calculated using the raw point force time histories (presented in blue). For clarity, low-pass filtered point force time histories were also used to reduce noise in the load direction time history (presented in green). A comparison of the magnitudes of the wind-tunnel predicted and flight test loads indicates that the wind tunnel data overpredicted the magnitude of the load by approximately 200 percent. The duration of the flight test event (highlighted in yellow) was approximately one fourth of the wind-tunnel predicted duration and the direction of the impulsive load was also not predicted correctly. The wind tunnel data indicated that the change in flow states should result in a loading directed at approximately 60 degrees azimuth. The flight test data indicates that the load initially is applied in the -150 degrees azimuth direction and changes direction to 60 degrees azimuth.

The direction and magnitude of the load produced during the transition from separated subsonic flow to attached supersonic flow is a function of the asymmetry of the flow transition around the vehicle circumference. For example, the largest load possible would occur if a continuous 180 degree arc section of the circumference changes flow states simultaneously from subsonic to supersonic, with the other half following later. The load direction would be a function of which section of the circumference transitioned first. The duration of the net load is governed by how long it takes the flow at the expansion corner to fully transition to supersonic attached flow around the entire vehicle circumference.

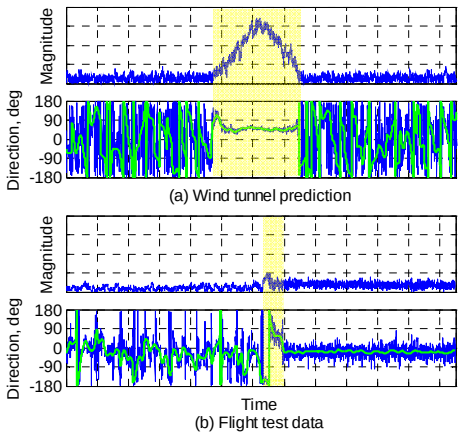

Figure 21. Comparison of integrated loads for wind tunnel prediction and flight test.

The transition from subsonic separated flow to supersonic attached flow downsteam of a cone-cylinder expansion corner is dependent on the local flow field. The flow field is influenced by factors such as vehicle geometry (protuberances, elastic deformation, etc.), vehicle attitude, atmospheric conditions, and the flight trajectory. The wind tunnel data derived impulsive load was based on a worst case scenario, which was measured at α=1° and β=0°. The best estimated trajectory of the Ares I-X FTV at the time of the impulsive load was approximately α=0.2° and β=-0.9°. This difference in vehicle attitude with respect to the free stream velocity may, in part, explain the differences noted in Figure 21.

The influence of vehicle attitude on the impulsive load was assessed by examining a buffet forcing function developed using wind tunnel data closest to the flight test α-β combination. Figure 22 presents the impulsive load generated by an alternating flow event based on a wind tunnel data measured at M=0.9, α=0.52, and β=-1.92. The magnitude of the new impulsive load is approximately twice that of the flight test load. The direction of the impulsive load was constant at -160 degrees for the duration of the entire event, instead of starting at 180 degrees and moving to 60 degrees as measured during the flight test. This difference in direction of the load is expected because of the flight test vehicle is accelerating while the wind tunnel model was tested at steady flight conditions.

The wind tunnel data derived event is created by a phenomenon where the flow over a portion of the vehicle circumference at the expansion corner changes states from subsonic detached state to a supersonic attached state, creating a net load at this vehicle station. Eventually the flow transitions back to the subsonic state returning the local vehicle loads back to equilibrium at a subsonic condition. The flight test vehicle measured event is created by the flow over a portion of the vehicle circumference changing states from subsonic flow to supersonic flow, but due to vehicle acceleration, the remainder of the vehicle circumference transitions to a supersonic flow state thereby returning the local vehicle loads back to equilibrium but at a supersonic condition.

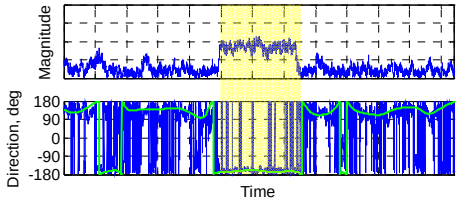

Figure 22. Integrated loads for wind tunnel data for model attitude of M=0.9, α=-0.52°, β=-1.93° (pitch =2°, roll=-75°.)

The duration of the impulsive load event was also overpredicted. Both predictions (Figures 21a and 22) seemed to overpredict the duration of the impulsive load by approximately 300 percent. This overprediction of the load duration is caused by the window size (based on vehicle first bending mode frequency) used to identify the most conservative alternating flow event. If this load duration was proven to result in significant overconservatism, then limiting the maximum duration of candidate events based on vehicle trajectory and refinements in wind tunnel data may be considered. The later refinement would require adjusting the wind tunnel test matrix once the presence of alternating flow is noted to provide a finer resolution of Mach numbers in the vicinity of the alternating flow flight condition in order more precisely identify the flight range affected by alternating flow.

IV. Conclusions

Wind tunnel tests of Ares I-X and Ares I rigid buffet models were conducted to develop transonic buffet forcing functions for the Ares I-X and Ares I launch vehicles. During the testing of the Ares I-X model, an alternating flow phenomenon was identified. The large transducer density in the vehicle region affected by this phenomenon, and the range of flight conditions and model configurations tested, provided a unique opportunity to study this phenomenon. The analysis of the Ares I and Ares I-X rigid buffet test data indicates:

1. Pressure time history $\Delta C_{p,rms}$ values, histograms, and cross-correlation plots are useful tools to help identify alternating flow separation and attachment phenomenon during wind tunnel testing and post-test analysis.
2. For the Ares I-X configuration, an alternating flow separation and attachment event occurred at the Crew Module-Service Module (CM-SM) junction for Mach numbers ranging from 0.88 to 0.92, depending on model angle of attack.
3. The Ares I model did not experience this phenomenon due to the presence of the ogive fairing around the Crew and Service Modules.
4. For the Ares I-X configuration, alternating flow is most prevalent at smaller (≤ 2°) model pitch angles. At these pitch angles, alternating flow was more organized, simultaneously affecting multiple transducers around the circumference.
5. Vehicle protuberances, especially the CM-SM umbilical, affect the magnitude and orientation of the impulsive loads created by alternating flow.
6. Flight data indicates that only a single impulsive load occurred as the flow at the CM-SM junction transitioned from a subsonic separated flow to a supersonic attached flow. Wind tunnel data overpredicted the magnitude and duration of this impulsive load.

Acknowledgements

The authors would like to thank Dr. Craig Streett of the Computational Aerosciences Branch at NASA Langley and Drs. Shin-Hsing Chen, James Canino, and Brian Sako of the Aerospace Corporation for their help in the analysis of the Ares I and Ares I-X Rigid Buffet Model data. The authors would also like to acknowledge the Ares Project Office at NASA Langley for their support of this work.

References

[1] Chevalier, H. and Robertson J., "Pressure Fluctuations Resulting from an Alternating Flow Separation and Attachment at Transonic Speeds". AEDC-TDR-63-204, November 1963.

[2]"Preliminary Report of Transient Pressures Measured on the 0.055 Scale Apollo Pressure Model (PSTL-1) in NAA Trisonic Wind Tunnel". North American Aviation, Inc. Space and Information Systems Division. Report NAS9-150, September, 1962.

[3]Jones, George W., Foughner, Jerome T., Jr., "Investigation of Buffet Pressures on Models of Large Manned Launch Vehicle Configurations". NASA TN-D-1663, May 1963.

[4]Rainey, Gerald A., "Progress on the Launch-Vehicle Buffeting Problem". *Journal of Spacecraft and Rockets*, Vol. 2, Num. 3, May-June 1965.

[5]Cockburn, J. A., Robertson, J. E. "Vibration Response of Spacecraft Shrouds to In-Flight Fluctuation Pressures". *Journal of Sound and Vibration*, Vol. 33, pp. 399-425. 22 Apr. 1974.

[6]Massey, S., and Chwalowski, P., "Computational Aeroelastic Analysis of Ares Crew Launch Vehicle Bi- Modal Loading". 27th AIAA Aerodynamic Measurement Technology and Ground Testing Conference, AIAA-2010-4373

[7]Streett, C. L., "Analysis of TDT AI-X Data Indicating Alternating-Flow Phenomena". Unpublished Ares Project presentation, March 2008.

[8]Piatak, D., Sekula, M., and Rausch, R., "Ares Launch Vehicle Transonic Buffet Testing and Analysis Techniques". 27th AIAA Aerodynamic Measurement Technology and Ground Testing Conference, AIAA-2010-4369.

[9]Piatak, D. J., et al, "Test Summary Document for the 3.5 Percent Ares I-X Rigid Buffet Model". ARES-AE-TA-0002, July 2008.

[10]Piatak, D. J., et al, "Test Summary Document for the 3.5 Percent Ares I Rigid Buffet Model". ARES-AE-TA-0012, March 2009.

[11]Piatak, D. J., et al, "Data Analysis and Results Document for the 3.5 Percent Ares I Rigid Buffet Model". ARES-AE-TA-0013, July 2009.